ACS chemical biology

Articles

pubs.acs.org/acschemicalbiology

Structural Basis for the Inhibition of HSP70 and DnaK Chaperones by Small-Molecule Targeting of a C-Terminal Allosteric Pocket

Julia I-Ju Leu,*[,†] Pingfeng Zhang,[‡,∥] Maureen E. Murphy,[⊥] Ronen Marmorstein,[‡,∥,§] and Donna L. George*[,†]

[†]Department of Genetics, [‡]Department of Biochemistry & Biophysics, Abramson Family Cancer Research Institute, Perelman School of Medicine, and [§]Department of Chemistry, University of Pennsylvania, Philadelphia, Pennsylvania 19104, United States

[∥]Program in Gene Expression and Regulation, and [⊥]Program in Molecular and Cellular Oncogenesis, The Wistar Institute, Philadelphia, Pennsylvania 19104, United States

Supporting Information

ABSTRACT: The stress-inducible mammalian heat shock protein 70 (HSP70) and its bacterial orthologue DnaK are highly conserved nucleotide binding molecular chaperones. They represent critical regulators of cellular proteostasis, especially during conditions of enhanced stress. Cancer cells rely on HSP70 for survival, and this chaperone represents an attractive new therapeutic target. We have used a structure−activity approach and biophysical methods to characterize a class of inhibitors that bind to a unique allosteric site within the C-terminus of HSP70 and DnaK. Data from X-ray crystallography together with isothermal titration calorimetry, mutagenesis, and cell-based assays indicate that these inhibitors bind to a previously unappreciated allosteric pocket formed within the non-ATP-bound protein state. Moreover, binding of inhibitor alters the local protein conformation, resulting in reduced chaperone−client interactions and impairment of proteostasis. Our findings thereby provide a new chemical scaffold and target platform for both HSP70 and DnaK; these will be important tools with which to interrogate chaperone function and to aid ongoing efforts to optimize potency and efficacy in developing modulators of these chaperones for therapeutic use.

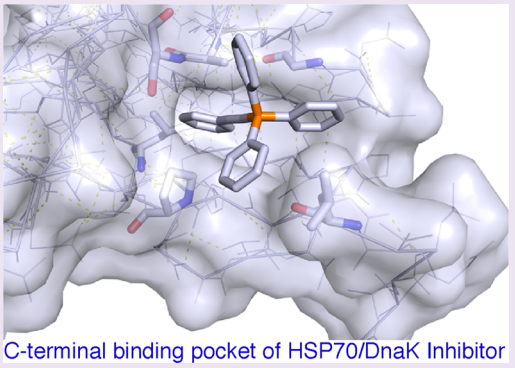

Maintaining protein homeostasis (proteostasis) is central to the survival of all cells, and altered protein quality control is characteristic of many human diseases. Critical components in this regulatory network are the mammalian stress-inducible heat shock protein-70 (inducible HSP70, also called HSPA1A or HSP72), as well as its evolutionarily conserved bacterial orthologue, DnaK.[1−5] These molecular chaperones coordinate key processes needed to maintain protein quality, especially under conditions of increased cellular stress. Their activities include protein folding, protein transport across membranes, modulating protein−protein interactions, and preventing a buildup of toxic protein aggregates. These molecular chaperones protect against proteotoxic stress, and not surprisingly, therefore, they are key survival proteins, especially for tumor cells.

HSP70 and DnaK are part of an evolutionarily conserved family of 70 kDa heat shock proteins.[1−5] The proteins have an approximately 44 kDa N-terminal nucleotide binding domain (NBD), followed by a conserved flexible linker, and an approximately 25 kDa C-terminal substrate binding domain (SBD). Each major domain contains several dynamic subdomains. These molecular chaperones transiently interact with a multitude of diverse substrates, or clients, by binding exposed hydrophobic regions of partially folded or unfolded proteins. ATP binding induces conformational changes in the NBD subdomains, promotes interdomain docking between the SBD and NBD, and promotes high on−off rates for the substrate.[6−9] In contrast, when ADP is bound to the chaperone, the NBD and SBD are more loosely held together by the linker region.[3,10] Allosteric communication between the NBD and SBD is critical to protein function; cycles of nucleotide binding and hydrolysis correlate with the binding and release of substrate, all of which are mediated by conformational changes in protein subdomains. The basic features of this allostery have been investigated for some time, often using *Escherichia coli* (*E. coli*) DnaK as a model. However, many key questions remain about the molecular details of this process, including whether inhibitors of these chaperones can interrupt this allosteric cycle.

Cancer cells are subject to an enhanced stress environment, and this promotes protein misfolding. Additionally, many cancer cells contain oncoproteins that contain missense mutations that can alter protein stability and conformation; thus, cancer cells are believed to be particularly dependent on the activities of HSP70 to maintain proteostasis. In support of this premise, HSP70 is constitutively expressed at elevated levels in most cancers, and silencing or inhibition of HSP70 has

Received: March 31, 2014
Accepted: August 22, 2014
Published: August 22, 2014

   dx.doi.org/10.1021/cb500236y | *ACS Chem. Biol.* 2014, 9, 2508−2516

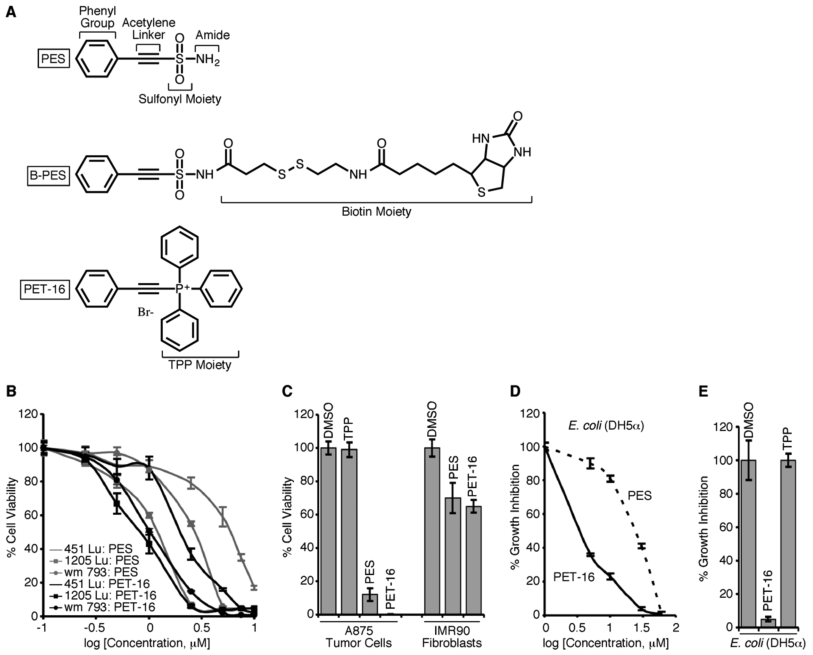

Figure 1. PET-16 is cytotoxic to human tumor cells and inhibits the growth of *E. coli*. (A) Chemical structures of PES, B-PES, and PET-16. The major functional groups are indicated. (B) MTT assays of human melanoma cell lines treated with the indicated concentrations of PES or PET-16 for 72 h. The corresponding cell survival is normalized to vehicle (DMSO) treatment. Average and standard deviation (s.d.) from three independent experiments are shown. (C) Human melanoma (A875) cells and nontransformed human (IMR90) fibroblasts were treated with DMSO, 10 μM PES, or 10 μM PET-16 for 24 h. The data shown are representative of four independent experiments. (D) Growth of *E. coli* DH5α treated with different concentrations of PES or PET-16 for 6 h at 43 °C. Error bars represent the s.d. of four independent experiments. (E) Growth of *E. coli* DH5α treated with DMSO, 30 μM PET-16, or 30 μM TPP for 6 h at 43 °C. Error bars represent the s.d. of four independent experiments.

been found to be cytotoxic to many tumor but not normal cells.[2,5,11,12] The preferential cytotoxicity of HSP70 inhibition for cancer cells is believed to relate to the modest to undetectable expression of this protein in normal cells, suggesting that there is a therapeutic index that can be exploited for preferential targeting of tumors. Indeed, HSP70 and DnaK have emerged as highly attractive targets for the development of new treatments for many human diseases, including microbial infections, neurodegenerative pathologies, and other disorders of protein folding. Despite a great deal of interest in the translational potential of small molecules that target these chaperones, identifying and characterizing effective modulators for basic research and therapeutic use has proven to be challenging. In particular, the dynamic nature and conformational flexibility of these molecular chaperones have complicated efforts to generate molecular data, which would inform structure-based design of improved inhibitors.[12−14] As a consequence, few selective inhibitors have been identified or are well-characterized at the structural and biophysical levels.[11−18]

We previously reported that the small molecule, 2-phenylethynesulfonamide (PES), and a chlorinated derivative (PES-Cl), interact with HSP70 and DnaK, and are cytotoxic to tumor cells in a manner that requires HSP70.[19−21] Unlike most other HSP70 inhibitors characterized to date, we identified the interaction site for PES and its derivatives as the C-terminal substrate binding domain of HSP70. This is in contrast with most other HSP70 inhibitors, which interact with the N-terminal nucleotide-binding domain.[13,18,27] The SBD is less conserved among HSP70 family members, and our data indicate that PES and its derivatives do not interact with the organelle-specific members of this family, GRP75 and GRP78 (BiP), which are required for the viability of all cells.[5,19] We have shown that these small molecules effectively inhibit HSP70 activities; importantly, this has now been confirmed by several other groups.[19−26] In this study, we carried out structure−activity relationship analyses to identify inhibitors with enhanced cytotoxicity and to define critical moieties that are required for the ability to inhibit HSP70 and DnaK chaperone activities. We report the identification of a new small molecule, triphenyl(phenylethynyl)phosphonium bromide (herein referred to as PET-16) that interacts with both HSP70 and DnaK, and alters *in vivo* function. We have successfully cocrystallized PET-16 with purified DnaK. Notably, our X-ray crystallographic data on PET-16 in complex with the C-terminal domain of DnaK, together with data from isothermal titration calorimetry and mutagenesis studies, now provide a model for how these compounds act as inhibitors of HSP70 as well as DnaK activity, by binding to a conserved region in these proteins and impeding substrate binding. These findings should facilitate efforts to further probe the physiologic functions of these molecular chaperones and support efforts to optimize potency and efficacy in developing HSP70 and DnaK modulators for therapeutic use.

RESULTS AND DISCUSSION

Functional Moieties and New Inhibitor Identification.

We previously reported that the small molecule PES ($C_8H_7NO_2S$, MW 181.21; Figure 1A) selectively binds to HSP70 and to DnaK, as demonstrated using "pull-down" assays with a biotin-tagged version of the molecule (B-PES, Figure 1A).[19,20] PES and a derivative, PES-Cl, also bind to *in vitro* translated HSP70, as well as to recombinant HSP70 and DnaK proteins, and this interaction is competed away with an untagged compound.[19−21] To identify important functional

dx.doi.org/10.1021/cb500236y | ACS Chem. Biol. 2014, 9, 2508−2516

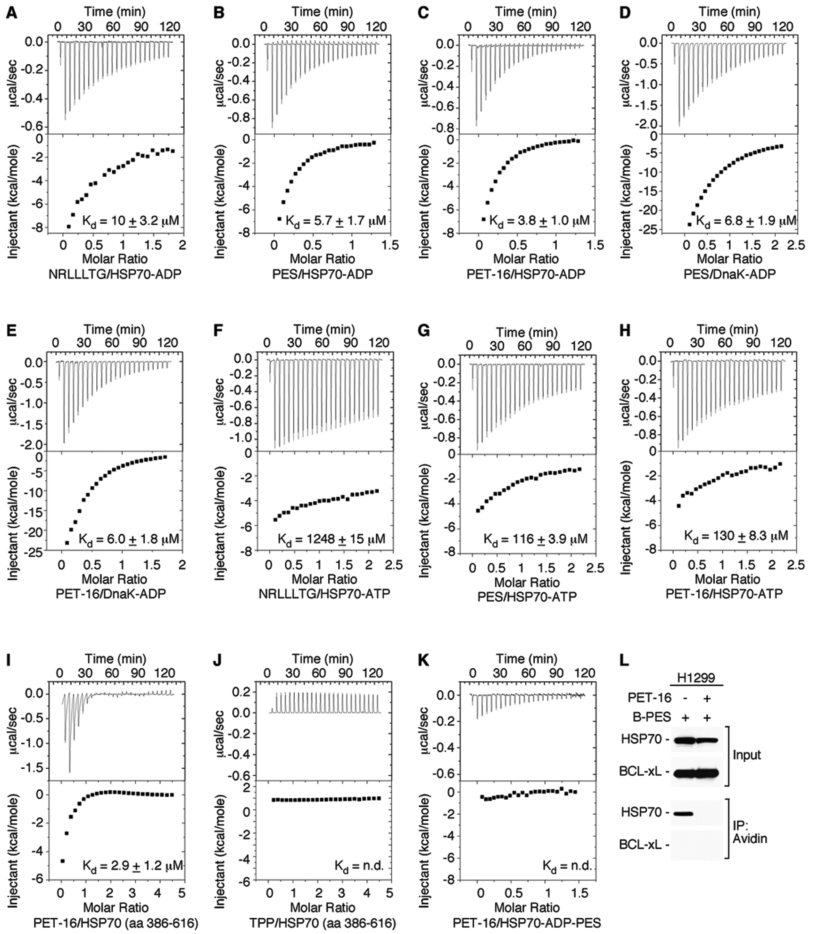

Figure 2. PET-16 binds directly to ADP-bound HSP70 and DnaK. (A–H) Representative ITC assays of the indicated compounds (NRLLLTG, PES or PET-16) with purified HSP70-ADP, DnaK-ADP, or HSP70-ATP proteins. The data shown are representative of three independent experiments. The reported dissociation constants are averages and standard deviations from three independent experiments. (I and J) Representative ITC binding curves obtained for the interaction between the HSP70 (aa 386–616) protein and PET-16 (I) or TPP (J). (K) HSP70 protein was preincubated with ADP and PES for 1 h. The mixture was titrated into the sample cell containing PET-16. The reported dissociation constants are averages and standard deviations from three independent experiments. (L) For competition studies, human lung carcinoma (H1299) cells were pretreated with DMSO or excess (8×) PET-16 for 1 h prior to the addition of 20 μM B-PES for 5 h and examined for the expression of HSP70 or BCL-xL. B-PES-containing complexes were captured by Avidin resins and immunoblotted either with anti-HSP70 or anti-BCL-xL antibody. As shown, PET-16 inhibits the subsequent interaction of HSP70 with B-PES.

determinants of inhibitor activity, we used a structure–activity relationship approach. As the biological read-out of this approach, we used the preferential cytotoxicity in transformed cells over normal, nontransformed cells. As proof-of-principle, a small-scale analysis of approximately 50 compounds was performed. This analysis pointed to the phenyl group (aromatic moiety) and acetylene linker as key features of selective PES-cytotoxicity in cancer cells (Figure 1A). Because HSP70 is present in many cellular compartments, including mitochondria, we designed a new molecule in which these key moieties are combined with a structural module, triphenylphosphine (TPP) bromide. The TPP moiety was selected in part because it has been shown to increase the cellular uptake of molecular probes across membranes.[28,29] The resulting molecule, triphenyl(phenylethynyl)phosphonium bromide ($C_{26}H_{20}BrP$; MW 443.327), the bromine salt of this compound, herein referred to as PET-16 (Figure 1A), exhibits enhanced cytotoxicity and increased solubility in aqueous solutions relative to the parental compound PES.

In cytotoxicity assays, concentrations of PET-16 that inhibit the viability of a broad range of tumor cell lines have little effect on nontransformed cells, including normal human fibroblasts and primary human melanocytes (Figure 1B and C; data not shown). For example, the IC_{50} for PET-16 in several of the melanoma cell lines examined was ~0.5–1.5 μM. In contrast, in primary melanocytes and fibroblasts the IC_{50} was over 30 μM (data not shown). Additionally, the TPP moiety alone has little discernible effect on the viability of mammalian tumor cells (Figure 1C), as previously reported.[28] Because bacteria rely on a functional DnaK system to survive stresses such as elevated temperatures, we next tested the effects of PET-16 on the phenotype of *E. coli*. We found that this small molecule impairs bacterial growth (Figure 1D and E); it also causes cell filamentation and reduced viability (data not shown), a phenotype that is identical to that of many DnaK mutants.[30,31] In contrast, we did not detect an effect of TPP on the growth of *E. coli* (Figure 1E).

To confirm that PET-16 binds directly to purified HSP70 and DnaK proteins, we used the technique of isothermal titration calorimetry (ITC). Full-length recombinant proteins of HSP70 (aa 1–641) and DnaK (aa 1–638) were first pretreated with either ADP or ATP to assess whether the

dx.doi.org/10.1021/cb500236y | *ACS Chem. Biol.* 2014, 9, 2508–2516

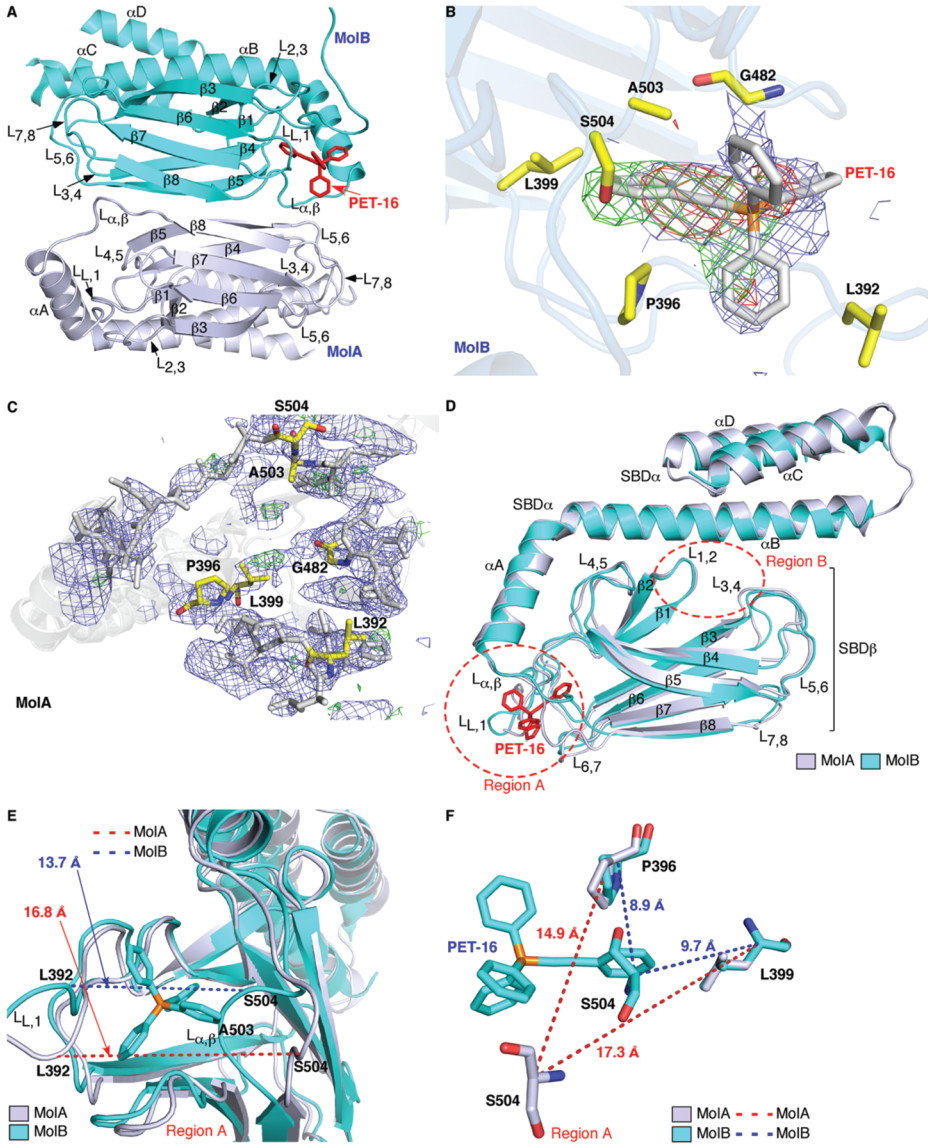

Figure 3. X-ray crystal structure of the DnaK-PET-16 complex. (A) Overall structure of the DnaK-PET-16 complex. The major domains and secondary structural elements are labeled. PET-16, in MolB, is shown in red. (B) Electron density map corresponding to PET-16 in the DnaK-PET-16 cocrystal structure. The $2F_o - F_c$ electron density map of the refined structure corresponding to PET-16 contoured at 1.0 σ is shown in blue. The $F_o - F_c$ difference map prior to introducing PET-16 into the model is contoured at 3.0 σ and shown in green; there is no contribution from PET-16 in this map. $F_o - F_c$ PET-16 omit map contoured at 3.0 σ is shown in red. The side chain of key PET-16 contacting residues and Gly482 are shown in stick format and labeled. The PET-16 compound is shown as a stick model in gray. Note that PET-16 binds to a pocket formed by strand β1 (L399) and loops LL,1 (L392, P396), L6,7 (G482), and Lα,β (A503 and S504). (C) Electron density map corresponding to MolA of the DnaK-PET-16 cocrystal structure. The $F_o - F_c$ map, corresponding to the PET-16 binding site in MolB, contoured at 3.0 σ, is shown in green. The $2F_o - F_c$ electron density map of strand β1 (L399) and loops LL,1 (L392, P396), L6,7 (G482), and Lα,β (A503 and S504) in MolA contoured at 1.5 σ is shown in blue. Key PET-16 contacting residues are shown in yellow stick format and labeled. The electron density corresponding to PET-16, as noted in Figure 3B, was not observed in the refined structure of MolA. (D) Structural alignment of MolA with MolB. The PET-16 compound is shown in red stick format and labeled. (E and F) Structural alignment of MolA with MolB. Structural differences noted in strand β1 and loops LL,1 and Lα,β of MolA and MolB are illustrated.

interaction of PET-16 might be influenced by different nucleotide-bound states of the protein. In addition, we also analyzed the interaction of HSP70 and DnaK with a well-studied peptide that serves as a "client protein" (NRLLLTG).[32,33] This peptide is well known to bind with high affinity when these chaperones are in the nucleotide-free and ADP-bound states but to have reduced affinity for the ATP-bound chaperone.[4,6,8,32−36] The ITC analyses revealed that PES and PET-16, similar to the peptide (Figure 2A), exhibit a strong preference for the ADP-bound form of HSP70 and DnaK, with K_d values of ∼3.8−6.8 μM (Figure 2B−E). These small molecules also interact with the nucleotide-free HSP70 protein with comparable affinity (Supporting Information, Figure S1 and data not shown). In contrast, the interaction of the peptide or inhibitor compounds with the ATP-bound form of HSP70 or DnaK was markedly reduced (Figure 2F−H). Thus, the ITC data support a model wherein PES and PET-16 preferentially target a "non-ATP-bound" form of HSP70 and DnaK; this finding is consistent with a previous suggestion that PES inhibits a "non-ATP-binding" form of

dx.doi.org/10.1021/cb500236y | ACS Chem. Biol. 2014, 9, 2508−2516

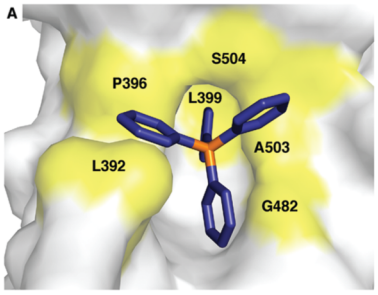

B

ADP-DnaK	PET-16 (K_d, μM)	PES (K_d, μM)
WT	6.0 ± 1.8	6.8 ± 1.9
L392D	37.9 ± 4.6	19.6 ± 1.4
P396L	53.5 ± 9.9	195.5 ± 21
L399R	69.7 ± 2.7	61.5 ± 0.9
G482D	38.1 ± 4.6	26.2 ± 1.4
A503D	77.5 ± 2.1	77.3 ± 1.0
S504A	49.6 ± 1.3	35.9 ± 1.8

ADP-HSP70	PET-16 (K_d, μM)	PES (K_d, μM)
WT	3.8 ± 1.0	5.7 ± 1.7
L394D	30.8 ± 0.6	26.6 ± 1.2
P398L	23.4 ± 1.2	24.3 ± 1.1
L401R	43.2 ± 9.9	48.5 ± 4.1
G484D	98.8 ± 5.1	97.1 ± 4.1
N505D	146.7 ± 6.5	107.5 ± 2.6
D506A	112.0 ± 3.8	144.5 ± 3.1

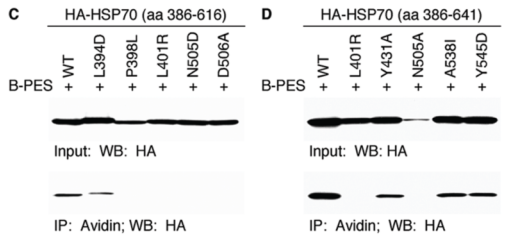

Figure 4. Mutation analyses support the DnaK-PET-16 cocrystal structure. (A) The binding pocket for PET-16 in the DnaK-PET-16 structure. The key residues that contact PET-16 in DnaK are highlighted and labeled. (B) PET-16 and PES bind directly to the C-terminal domain of ADP-bound DnaK and HSP70. ITC-derived binding constants (K_d values) from assays of PES and PET-16 incubated with wild-type and mutated full-length ADP-DnaK (top panel) and ADP-HSP70 proteins (bottom panel). The reported dissociation constants are averages and standard deviations from three independent experiments. (C and D) Pull-down assays using H1299 cells transfected with the indicated HA-tagged HSP70 constructs followed by treatment with 20 μM B-PES for 5 h. B-PES-containing complexes were captured by avidin beads, eluted, and detected with an anti-HA antibody following immunoblotting. Input is shown on the top panel; immunoprecipitation (IP) with avidin is depicted on the bottom.

HSP70 involved in the activation of apo-neuronal nitric oxide synthase.[24] It is worth noting that crystallographic and NMR analyses indicate that the ADP-bound- and nucleotide-free-forms of DnaK are conformationally similar to each other and distinct from the ATP-bound state.[4,7,9,10,32,36]

Our ITC results contrast with a recent report that failed to detect a specific interaction between PES and HSP70 using ITC.[37] We attribute this discrepancy to the quite disparate experimental conditions employed, which are detailed and discussed in Supporting Information, Methods. Indeed, by optimizing the ITC protocol conditions, we are readily able to detect a direct, specific interaction between the small molecules and HSP70 and DnaK. Our ITC data are further supported by the identification of point mutants of HSP70 and DnaK that interfere with the binding of PES and PET-16, as presented below.

The ITC binding curves support a stoichiometry whereby one molecule of PES or PET-16 binds in a complex containing two molecules of ADP-bound HSP70 or DnaK (Figure 2B–E). Because our previous investigations showed that the small molecules directly bind to the C-terminal region of HSP70 (residues 386–616) and DnaK (residues 389–607),[19−21] recombinant proteins containing these domains also were employed in ITC experiments. We found that PET-16 also binds to the C-terminal domain of HSP70, exhibiting a K_d of ∼2.9 μM (Figure 2I). In contrast, the TPP moiety alone does not bind to either HSP70 or DnaK SBD (Figure 2J and data not shown). Using ITC analyses, we also discovered that preincubation of HSP70 with PES markedly reduces the binding affinity of the protein for PET-16 (Figure 2K). Similarly, presaturation of HSP70 with PET-16 also impairs the interaction of this protein with PES (data not shown). These data are consistent with the hypothesis that these chemically related compounds likely bind to the same site of the HSP70 protein. To further assess this possibility *in vivo*, we employed biotin-tagged PES (B-PES, Figure 1A) in a pull-down assay, similar to our previously described investigations.[19−21] In this assay, cultured tumor cells were pretreated with PET-16 for 1 h prior to the addition of biotin-tagged-PES (B-PES). B-PES-containing complexes were then captured using Avidin beads and then examined for the presence of HSP70 by immunoblotting. We found that pretreating cells with PET-16 clearly reduced the amount of HSP70 found in complex with B-PES (Figure 2L), as suggested by the ITC data (Figure 2K).

Crystallographic Data on the DnaK-PET-16 Complex. To better understand the structural basis for how these small molecules target HSP70 and DnaK, we sought to generate crystals of protein−inhibitor complexes suitable for analysis by X-ray crystallography. We obtained crystals of the SBD of DnaK (aa 389–607) in the presence of PET-16 in the $P4_32_12$ space group. The PET-16-DnaK crystals contained two molecules [referred to as molecule A (MolA) and molecule B (MolB)] per asymmetric unit cell and diffracted to 3.45 Å, which was also the refinement limit (Figure 3A and Supporting Information, Table S1). During and following refinement, additional difference density was detected in MolB (Figure 3B and Supporting Information, Figure S2A–E), but not in MolA (Figure 3C), of the DnaK, occupying a binding pocket formed by residues in strand β1 (L399) and loops LL,1 (L392 and P396), L6,7 (G482), and Lα,β (A503 and S504). This additional electron density in MolB was modeled as PET-16; we noted the electron-rich phosphine in the region of greatest electron density, the phenyl group and acetylene linker pointing into the binding pocket, and the TPP located out toward the solvent. This was consistent with additional rounds of crystallographic refinement (Figure 3B and Supporting Information, Figure S2A–E). A superposition of MolB to MolA of the DnaK-PET-16 structure reveals that the two

dx.doi.org/10.1021/cb500236y | ACS Chem. Biol. 2014, 9, 2508–2516

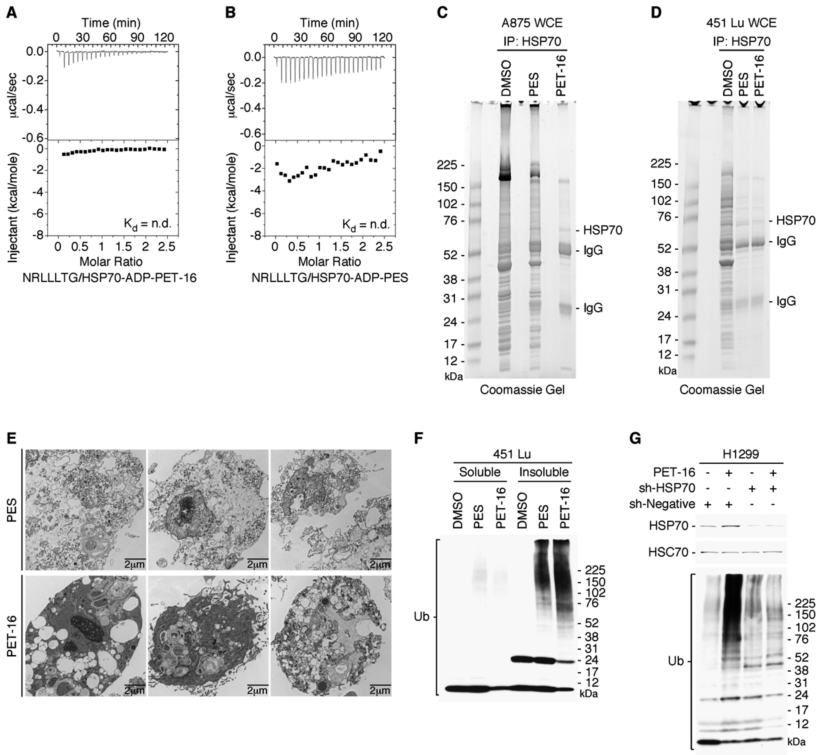

Figure 5. PET-16 impairs chaperone−client interaction and proteostasis. (A and B) Representative ITC-binding isotherms were recorded for the full-length recombinant human HSP70 proteins pretreated for 1 h with ADP and PET-16 (A) or with ADP and PES (B) and then titrated into a solution of substrate peptide NRLLLTG. The data shown here are representative of three independent experiments. (C and D) Whole-cell extracts (WCE) prepared from human melanoma A875 (C) or 451 Lu (D) cells treated with DMSO, PES, or PET-16 were immunoprecipitated using an anti-HSP70 antibody. The excised band of ∼70 kDa shown in the Coomassie gel is HSP70, as confirmed by liquid chromatography−tandem mass spectrometry analysis. (E) EM analysis provides evidence of altered autophagy in PET-16 treated tumor cells, with the presence of autophagosomes, accumulation of vacuoles, and the appearance of granular and aggregated masses. Note the general absence of obvious nuclei in PET-16 treated tumor cells. (F) Human melanoma 451 Lu cells were treated with DMSO, PES, or PET-16 for 24 h. Cells were harvested in 1% NP40-containing lysis buffer, fractionated into detergent-soluble and detergent-insoluble preparations, and assayed by Western blot for ubiquitin. (G) Human H1299 lung carcinoma cells, transfected with a negative shRNA (sh-Negative) or with HSP70 shRNAs (sh-HSP70), were treated with DMSO or PET-16, as indicated. Proteins were assayed by Western blot for ubiquitin in the detergent-insoluble fraction and for HSP70 and HSC70 in the detergent-soluble fraction.

molecules in each asymmetric unit exhibit distinct conformations (Figure 3D). Specifically, in MolB, the interactions among PET-16, strand β1, loop LL,1, and loop Lα,β bring residues L392, P396, and L399 closer to residue S504 by ∼3.1, 6.0, and 7.6 Å, respectively, relative to their positions in MolA (Figure 3E and F). The model of PET-16 binding to only one of two molecules in the asymmetric unit cell of the crystals is consistent with the 1:2 stoichiometry observed in the ITC analyses (Figure 2C and E), suggesting that the observed crystallographic DnaK dimer that presents only one PET-16 binding site also occurs in solution. Other crystal structures have been reported in which ligands bind to only one of the two protomers of an asymmetric crystal cell.[38−40] This includes, for example, the inositol 1,4,5-trisphosphate ($InsP_3$) as well as the BRAF inhibitor PLX4032.[38,39] We then focused attention on the DnaK molecule containing the modeled PET-16 (MolB); this complex is referred to as DnaK-PET-16.

Mutation Analyses Validate the Site of Inhibitor Interaction. Amino acids L392, P396, L399, G482, A503, and S504 are key residues that contact PET-16 in DnaK (Figure 4A). The former four residues are conserved and correspond to residues L394, P398, L401, and G484 in HSP70. Like A503 and S504 in DnaK, residues N505 and D506 in HSP70 also form the entrance to a conserved inhibitor binding pocket.[41] Our analysis indicates that PET-16 binds to this binding cleft (Region A, Figures 3D and 4A), which is distinct from the canonical substrate-binding pocket (Region B, Figure 3D). Mutation analysis provided additional experimental support for this inhibitor binding location. Specifically, single point mutants were introduced in the context of a full-length DnaK protein or at the corresponding residues of HSP70. The DnaK mutations tested include L392D, P396L, L399R, G482D, A503D, and S504A; those in HSP70 were L394D, P398L, L401R, G484D, N505D, and D506A. ITC analysis indicated that the presence of each of these mutations markedly reduced the affinity of these proteins for PET-16 as well as PES (Figure 4B).

We next tested whether the mutations described above would similarly impair the binding of PES to HSP70 in cultured cells. To do so, we generated constructs encoding hemagglutinin (HA) epitope-tagged recombinant HSP70 (residues 386−616 or residues 386−641) containing individual point mutations; some of these were predicted to alter critical contact residues, whereas others were chosen in unbiased fashion. In sum, the HSP70 mutants L394D, P398L, L401R, Y431A, N505A, N505D, D506A, A538I, and Y545D were generated. Each construct was transiently expressed in cultured tumor cells that were treated with a biotin-tagged version of PES (B-PES).

dx.doi.org/10.1021/cb500236y | ACS Chem. Biol. 2014, 9, 2508−2516

Cell lysates were then assayed for the interaction between B-PES and mutant HA-HSP70 proteins in pull-down assays using Avidin resin, followed by immunoblotting using anti-HA antibodies (Figure 4C and D). The results demonstrate that mutation of HSP70 residues P398, L401, N505, and D506 each result in a reduced interaction between B-PES and HSP70 (Figure 4C and D). In contrast, mutation of residues Y431A, A538I, and Y545D does not discernibly alter binding (Figure 4D). In sum, the data obtained in these mutagenesis studies support the information provided by the X-ray crystal structure of DnaK-PET-16; they suggest that residues L394, P398, L401, G484, N505, and D506 in HSP70, as well as the corresponding residues in DnaK, represent important elements for the interaction of PET-16 and PES.

PET-16 Binding Pocket Is Present in the ADP-Bound Protein. Full-length DnaK structures, bound to either ADP or ATP, have recently been determined.[6−10] To gain additional insight regarding how the interaction between PET-16 and DnaK may impact the DnaK SBD, we overlaid structurally corresponding Cα atoms of the SBD of DnaK-PET-16 with the following reported structures: a full-length ADP-bound DnaK NMR structure (PDB code 2KHO)[10] and two full-length ATP-bound DnaK X-ray structures (PDB codes 4JN4 and 4B9Q)[7,9] (Supporting Information, Figure S3). From this analysis, we noted that the crystal structure of DnaK-PET-16 is substantially different from the ATP-DnaK-SBD structures (an overall Cα rmsd = 26.243 and 26.039 Å for 4JN4 and 4B9Q, respectively). In the presence of PET-16, helices A and B of the SBDα do not form a continuous helix as noted in the DnaK-ATP structures (Supporting Information, Figure S3B and C). In contrast, the SBDβ domain of the DnaK-PET-16 structure is conformationally similar to the ADP-bound DnaK structure, except in loops LL,1 and Lα,β where PET-16 interacts. As shown, residue L392 in loop LL,1 and residue S504 in Lα,β are closer together by ∼7.7 Å relative to the corresponding residues in the ADP-state in the absence of PET-16 (Supporting Information, Figure S3A).

These combined observations suggest that the location of residues comprising the PET-16-binding-cavity is strongly influenced by allosteric changes in the protein. Indeed, topological analysis revealed that the binding cleft occupied by PET-16 is readily apparent in the ADP-state (Supporting Information, Figure S3D) but is not available in the reported crystal structures of the ATP-form (Supporting Information, Figure S3E and F). This clear structural difference between the ADP-bound and ATP-bound forms of the protein is consistent with the preferential binding of PES and PET-16 to the non-ATP-bound conformation.

PET-16 Inhibits HSP70−Client Interactions, Both *in Vitro* and *in Vivo*, and Impairs Cellular Proteostasis. We next determined whether prior exposure to PES or PET-16 modulates the binding of peptide substrate to HSP70. On the basis of ITC analyses (Figure 2A), NRLLLTG and ADP-bound HSP70 formed a 1:1 complex with a K_d of ∼10 μM. However, we found that presaturation of ADP-bound HSP70 with either PES or PET-16 markedly reduces the affinity of HSP70 for the peptide substrate NRLLLTG (Figure 5A and B). To extend these analyses, we determined whether the binding of HSP70 to PET-16 similarly alters HSP70−client interactions *in vivo*. We treated tumor cell lines with PET-16, affinity purified HSP70−client complexes, and examined HSP70−substrate interactions by SDS−PAGE followed by Coomassie staining. The results show that PET-16 markedly reduces the number of polypeptides that coimmunoprecipitate with endogenous HSP70 (Figure 5C and D). Such a marked reduction in HSP70−client interaction would be predicted to disrupt overall cellular protein quality control and induce proteotoxic stress.

The chaperone activities of HSP70 are closely coordinated with the autophagy-lysosome and proteasome pathways, which mediate protein turnover and disposal.[42−44] These pathways act to prevent the accumulation of misfolded and aggregated proteins in cells. A dysregulation of the protein quality control machinery can lead to a toxic persistence of misfolded proteins. Indeed, electron microscopy confirms that tumor cells treated with PET-16, like PES, contain multiple double-membrane and single-membrane structures and multiple vacuoles, consistent with impaired autophagy. Some of the vacuoles harbor recognizable cytoplasmic content as well as amorphous, membranous, aggregated, or granular masses (Figure 5E). Consistent with this finding, immunoblot analysis of lysates from PET-16 treated cells reveals an increase in the abundance of a heterogeneous population of ubiquitinated polypeptides, especially in the detergent insoluble cell fraction (Figure 5F). Since ubiquitin often serves as a covalent tag to mark proteins for degradation, an accumulation of ubiquitinated polypeptides is indicative of impaired proteostasis.

We next investigated the requirement for HSP70 for the ability of PET-16 to cause accumulation of ubiquitinated polypeptides. In previous work,[19] we described a set of shRNAs that could successfully silence HSP70, leading to markedly reduced cellular HSP70 abundance and a concomitant abrogation of PES-mediated cell death in tumor cells. Accordingly, we used a similar approach here. Because treating cells with PET-16 leads to increased cellular levels of HSP70, this can complicate efforts to effectively reduce HSP70 protein abundance, especially over long periods. Nonetheless, using four distinct shRNA sequences, HSP70 expression was selectively reduced in the transfected cells, and this resulted in a clear decrease in the accumulation of ubiquitinated polypeptides in response to PET-16 (Figure 5G). Note that the HSP70 shRNAs were selective and had no effect on HSC70 expression (Figure 5G). These results further support HSP70 as the critical target of PET-16 action.

Concluding Remarks. Stress-inducible HSP70 and DnaK proteins are critical mediators of protein quality control that have been implicated in several human diseases. The chaperoning activities of HSP70 and DnaK are regulated by conformational changes associated with interconversion among ATP-bound, ADP-bound, and nucleotide-free states; these are influenced by substrate binding and release, cofactor interactions, and physiologic conditions. Agents or events that interfere with conformational flexibility are predicted to impair chaperone function. Here, we generated crystals of the C-terminal domain of DnaK, both alone and in complex with either a peptide substrate or inhibitor (Supporting Information, Tables S1, S2, and S4). Our data provide evidence that the small molecule PET-16, described herein, represents an inhibitor class that binds within a conserved C-terminal binding pocket of the HSP70 and DnaK proteins; this pocket is distinct from the site of chaperone−substrate interaction and is evident only in the non-ATP-bound protein conformation. Changes in local protein environment are apparent in the PET-16-bound versus unbound state (Figure 3 and Supporting Information, Figures S3−S5). Previous investigations, using either mutation analyses or structural studies, have established the importance of the residues within loops LL,1, L6,7, and Lα,β of DnaK for

allosteric coupling of NBD and SBD, the interaction of chaperone with the critical HSP40 cochaperone, or overall bacterial viability.[6,8,9,45,46] It is reasonable to suggest, therefore, that by binding to this well-conserved C-terminal binding pocket, the inhibitors disrupt the conformational flexibility between the SBDα-SBDβ and/or NBD-SBD interface needed for allosteric regulation and proper chaperone function. In support of this premise, we find that these small molecules reduce the survival of mammalian tumor cells, impair bacterial growth, modulate cellular interactions between HSP70 and cochaperones, and alter interactions with substrates. The combined data are consistent with the following working hypothesis: by locking (or prolonging) HSP70 and DnaK in a particular conformational state, these small molecules negatively impact the substrate binding/release cycle of HSP70 and DnaK allostery. Indeed, the inhibitors may function in a manner that may impart a "gain-of-function" phenotype, resulting in the accumulation of aggregates and misfolded proteins in detergent insoluble cell fractions, possibly in association with the chaperone itself. Also, while PES and PET-16 share many properties, ongoing investigations point to differences as well. It is anticipated that the various mutant forms of DnaK and HSP70 generated in this investigation, as well as the inhibitor compounds described, will have direct utility for future *in vitro* and *in vivo* studies aimed at dissecting the role of the binding region and particular amino acid residues in chaperone activities, such as allostery regulation, substrate binding/release, and interaction with particular cochaperone mediators. The new information obtained provides a timely and useful molecular platform to inform the structure-based design of additional modulators that preferentially target the C-terminal binding pocket of HSP70 and DnaK proteins to alter the chaperone−client network, with potential application to human disease. Our work represents an important step toward the goal of moving these compounds into therapeutic use.

■ ASSOCIATED CONTENT

Supporting Information

Methods, PET-16 binding directly to the nucleotide-free HSP70 protein; data collection and refinement statistics for the DnaK-PET-16 structure, unliganded DnaK structures, and the substrate-bound DnaK structure; X-ray crystal structure of the DnaK-PET-16 complex; summary of comparative analyses; and PET-16 binding modulating the DnaK structure relative to the unliganded form and the substrate-bound protein. This material is available free of charge via the Internet at http://pubs.acs.org.

Accession Codes

The atomic coordinates and structure factors have been deposited in the Protein Data Bank with the accession numbers: 4R5G (DnaK-PET-16), 4R5J (DnaK-SBD-A), 4R5K (DnaK-SBD-B), 4R5L (DnaK-SBD-C), and 4R5I (DnaK-NRLLLTG-A).

■ AUTHOR INFORMATION

Corresponding Authors

*(J.I.L.) Phone: 215-898-5032. E-mail: leu@mail.med.upenn.edu.

*(D.L.G.) Phone: 215-898-5032. E-mail: georged@mail.med.upenn.edu

Notes

The authors declare no competing financial interest.

■ ACKNOWLEDGMENTS

This work was supported by US Public Health Service National Institutes of Health Grants R01CA139319 (to M.E.M.) and PO1CA114046 (to J.I.L., M.E.M., R.M., and D.L.G.). Portions of the work used core facilities funded in part by the Abramson Cancer Center Support Grant (P30CA016520).

■ REFERENCES

(1) Mayer, M.-P., and Bukau, B. (2005) Hsp70 chaperones: cellular functions and molecular mechanism. *Cell. Mol. Life Sci. 62*, 670−684.

(2) Daugaard, M., Rohde, M., and Jäättelä, M. (2007) The heat shock protein 70 family: highly homologous proteins with overlapping and distinct functions. *FEBS Lett. 581*, 3702−3710.

(3) Kim, Y.-E., Hipp, M.-S., Hayer-Hartl, A.-B.-M., and Hartl, F.-U. (2013) Molecular chaperone functions in protein folding and proteostasis. *Annu. Rev. Biochem. 82*, 323−355.

(4) Mayer, M.-P. (2013) Hsp70 chaperone dynamics and molecular mechanism. *Trends Biochem. Sci. 38*, 507−514.

(5) Murphy, M.-E. (2013) The HSP70 family and cancer. *Carcinogenesis 34*, 1181−1188.

(6) Swain, J.-F., Dinler, G., Sivendran, R., Montgomery, D.-L., Stotz, M., and Gierasch, L.-M. (2007) Hsp70 chaperone ligands control domain association via an allosteric mechanism mediated by the interdomain linker. *Mol. Cell 26*, 27−39.

(7) Kityk, R., Kopp, J., Sinning, I., and Mayer, M.-P. (2012) Structure and dynamics of the ATP-bound open conformation of Hsp70 chaperones. *Mol. Cell 48*, 863−874.

(8) Zhuravleva, A., Clerico, E.-M., and Gierasch, L.-M. (2012) An interdomain energetic tug-of-war creates the allosterically active state in Hsp70 molecular chaperones. *Cell 151*, 1296−1307.

(9) Qi, R., Sarbeng, E.-B., Liu, Q., Le, K. Q., Xu, X., Xu, H., et al. (2013) Allosteric opening of the polypeptide-binding site when an Hsp70 binds ATP. *Nat. Struct. Mol. Biol. 20*, 900−907.

(10) Bertelsen, E.-B., Chang, L., Gestwicki, J.-E., and Zuiderweg, E.-R. (2009) Solution conformation of wild-type E. coli Hsp70 (DnaK) chaperone complexed with ADP and substrate. *Proc. Natl. Acad. Sci. U.S.A. 106*, 8471−8476.

(11) Brodsky, J.-L., and Chiosis, G. (2006) Hsp70 molecular chaperones: emerging roles in human disease and identification of small molecule modulators. *Curr. Top. Med. Chem. 6*, 1215−1225.

(12) Powers, M.-V., Jones, K., Barillari, C., Westwood, I., van Montfort, R.-L., and Workman, P. (2010) Targeting HSP70: the second potentially druggable heat shock protein and molecular chaperone. *Cell Cycle 9*, 1542−1550.

(13) Rodina, A., Patel, P.-D., Kang, Y., Patel, Y., Baaklini, I., Wong, M.-J., et al. (2013) Identification of an allosteric pocket on human Hsp70 reveals a mode of inhibition of this therapeutically important protein. *Chem. Biol. 20*, 1469−1480.

(14) Kang, Y., Taldone, T., Patel, H.-J., Patel, P.-D., Rodina, A., Gozman, A., et al. (2014) Heat shock protein 70 inhibitors. 1. 2,5′-Thiodipyrimidine and 5-(Phenylthio)pyrimidine Acrylamides as irreversible binders to an allosteric site on heat shock protein 70. *J. Med. Chem. 57*, 1188−1207.

(15) Cellitti, J., Zhang, Z., Wang, S., Wu, B., Yuan, H., Hasegawa, P., et al. (2009) Small molecule DnaK modulators targeting the beta-domain. *Chem. Biol. Drug. Des. 74*, 349−357.

(16) Patury, S., Miyata, Y., and Gestwicki, J.-E. (2009) Pharmacological targeting of the Hsp70 chaperone. *Curr. Top. Med. Chem. 9*, 1337−1351.

(17) Rérole, A.-L., Gobbo, J., De Thonel, A., Schmitt, E., Pais de Barros, J.-P., Hammann, A., et al. (2011) Peptides and aptamers targeting HSP70: a novel approach for anticancer chemotherapy. *Cancer Res. 71*, 484−495.

(18) Chang, L., Miyata, Y., Ung, P.-M., Bertelsen, E.-B., McQuade, T.-J., Carlson, H.-A., et al. (2011) Chemical screens against a

reconstituted multiprotein complex: myricetin blocks DnaJ regulation of DnaK through an allosteric mechanism. *Chem. Biol. 18*, 210−221.
(19) Leu, J.-I., Pimkina, J., Frank, A., Murphy, M.-E., and George, D.-L. (2009) A small molecule inhibitor of inducible heat shock protein 70. *Mol. Cell 36*, 15−27.
(20) Leu, J.-I., Pimkina, J., Pandey, P., Murphy, M.-E., and George, D.-L. (2011) HSP70 inhibition by the small-molecule 2-phenylethynesulfonamide impairs protein clearance pathways in tumor cells. *Mol. Cancer Res. 9*, 936−947.
(21) Balaburski, G.-M., Leu, J.-I., Beeharry, N., Hayik, S., Andrake, M.-D., Zhang, G., et al. (2013) A modified HSP70 inhibitor shows broad activity as an anticancer agent. *Mol. Cancer Res. 11*, 219−229.
(22) Iwasaki, S., Kobayashi, M., Yoda, M., Sakaguchi, Y., Katsuma, S., Suzuki, T., et al. (2010) Hsc70/Hsp90 chaperone machinery mediates ATP-dependent RISC loading of small RNA duplexes. *Mol. Cell 39*, 292−299.
(23) Iki, T., Yoshikawa, M., Nishikiori, M., Jaudal, M.-C., Matsumoto-Yokoyama, E., Mitsuhara, I., et al. (2010) In vitro assembly of plant RNA-induced silencing complexes facilitated by molecular chaperone HSP90. *Mol. Cell 39*, 282−291.
(24) Morishima, Y., Lau, M., Peng, H.-M., Miyata, Y., Gestwicki, J.-E., Pratt, W.-B., et al. (2011) Heme-dependent activation of neuronal nitric oxide synthase by cytosol is due to an Hsp70-dependent, thioredoxin-mediated thiol-disulfide interchange in the heme/substrate binding cleft. *Biochemistry 50*, 7146−7156.
(25) Kwak, P.-B., and Tomari, Y. (2012) The N domain of argonaute drives duplex unwinding during RISC assembly. *Nat. Struct. Mol. Biol. 19*, 145−151.
(26) Liu, B., Han, Y., and Qian, S.-B. (2013) Cotranslational response to proteotoxic stress by elongation pausing of ribosomes. *Mol. Cell 49*, 453−463.
(27) Rousaki, A., Miyata, Y., Jinwal, U.-K., Dickey, C.-A., Gestwicki, J.-E., and Zuiderweg, E. R. (2011) Allosteric drugs: the interaction of antitumor compound MKT-077 with human Hsp70 chaperones. *J. Mol. Biol. 411*, 614−632.
(28) Millard, M., Pathania, D., Shabaik, Y., Taheri, L., Deng, J., and Neamati, N. (2010) Preclinical evaluation of novel triphenylphosphonium salts with broad-spectrum activity. *PLoS One 5*, e13131.
(29) Smith, R.-A., Hartley, R.-C., and Murphy, M.-P. (2011) Mitochondria-targeted small molecule therapeutics and probes. *Antioxid. Redox Signaling 15*, 3021−3038.
(30) Bukau, B., and Walker, G.-C. (1989) Delta dnaK52 Mutants of *Escherichia coli* have defects in chromosome segregation and plasmid maintenance at normal growth temperatures. *J. Bacteriol. 171*, 6030−6038.
(31) McCarty, J.-S., and Walker, G.-C. (1994) DnaK mutants defective in ATPase activity are defective in negative regulation of the heat shock response: expression of mutant DnaK proteins results in filamentation. *J. Bacteriol. 176*, 764−780.
(32) Zhu, X., Zhao, X., Burkholder, W.-F., Gragerov, A., Ogata, C.-M., Gottesman, M.-E., et al. (1996) Structural analysis of substrate binding by the molecular chaperone DnaK. *Science 272*, 1606−1614.
(33) Wang, H., Kurochkin, A.-V., Pang, Y., Hu, W., Flynn, G.-C., and Zuiderweg, E.-R. (1998) NMR solution structure of the 21 kDa chaperone protein DnaK substrate binding domain: a preview of chaperone-protein interaction. *Biochemistry 37*, 7929−7940.
(34) Pellecchia, M., Montgomery, D.-L., Stevens, S.-Y., Vander Kooi, C.-W., Feng, H.-P., Gierasch, L.-M., et al. (2000) Structural insights into substrate binding by the molecular chaperone DnaK. *Nat. Struct. Biol. 7*, 298−303.
(35) Aprile, F.-A., Dhulesia, A., Stengel, F., Roodveldt, C., Benesch, J.-L., Tortora, P., et al. (2013) Hsp70 oligomerization is mediated by an interaction between the interdomain linker and the substrate-binding domain. *PLoS One 8*, e67961.
(36) Mayer, M.-P., Schröder, H., Rüdiger, S., Paal, K., Laufen, T., and Bukau, B. (2000) Multistep mechanism of substrate binding determines chaperone activity of Hsp70. *Nat. Struct. Biol. 7*, 586−593.
(37) Schlecht, R., Scholz, S.-R., Dahmen, H., Wegener, A., Sirrenberg, C., Musil, D., et al. (2013) Functional analysis of hsp70 inhibitors. *PLoS One 8*, e78443.
(38) Lin, C.-C., Baek, K., and Lu, Z. (2011) Apo and $InsP_3$-bound crystal structures of the ligand-binding domain of an $InsP_3$ receptor. *Nat. Struct. Mol. Biol. 18*, 1172−1174.
(39) Bollag, G., Hirth, P., Tsai, J., Zhang, J., Ibrahim, P.-N., Cho, H., et al. (2010) Clinical efficacy of a RAF inhibitor needs broad target blockade in BRAF-mutant melanoma. *Nature 467*, 596−599.
(40) Tsai, J., Lee, J.-T., Wang, W., Zhang, J., Cho, H., Mamo, S., et al. (2008) Discovery of a selective inhibitor of oncogenic B-Raf kinase with potent antimelanoma activity. *Proc. Natl. Acad. Sci. U.S.A. 105*, 3041−3046.
(41) Zhang, P., Leu, J.-I., Murphy, M.-E., George, D.-L., and Marmorstein, R. (2014) Crystal structure of the stress-inducible human heat shock protein 70 substrate-binding domain in complex with peptide substrate. *PLoS One 9*, e103518.
(42) Nylandsted, J., Gyrd-Hansen, M., Danielewicz, A., Fehrenbacher, N., Lademann, U., Høyer-Hansen, M., et al. (2004) Heat shock protein 70 promotes cell survival by inhibiting lysosomal membrane permeabilization. *J. Exp. Med. 200*, 425−435.
(43) Ryhänen, T., Hyttinen, J.-M., Kopitz, J., Rilla, K., Kuusisto, E., Mannermaa, E., et al. (2009) Crosstalk between Hsp70 molecular chaperone, lysosomes and proteasomes in autophagy-mediated proteolysis in human retinal pigment epithelial cells. *J. Cell. Mol. Med. 13*, 3616−3631.
(44) Kirkegaard, T., Roth, A.-G., Petersen, N.-H., Mahalka, A.-K., Olsen, O.-D., Moilanen, I., et al. (2010) Hsp70 stabilizes lysosomes and reverts Niemann-Pick disease-associated lysosomal pathology. *Nature 463*, 549−553.
(45) Liu, Q., and Hendrickson, W.-A. (2007) Insights into Hsp70 chaperone activity from a crystal structure of the yeast Hsp110 Sse1. *Cell 131*, 106−120.
(46) Kumar, D.-P., Vorvis, C., Sarbeng, E.-B., Cabra Ledesma, V.-C., Willis, J.-E., and Liu, Q. (2011) The four hydrophobic residues on the Hsp70 inter-domain linker have two distinct roles. *J. Mol. Biol. 411*, 1099−1113.